Radio Science

RESEARCH ARTICLE
10.1029/2019RS006871

Key Points:
- An effective method is presented for mutual coupling reduction that is based on metasurface isolator for MIMO and SAR applications
- Effectiveness of the metasurface is demonstrated with a 2x2 antenna array that operates over six frequency sub-bands in X, Ku and K-bands
- The maximum improvement achieved in attenuating mutual coupling is 8.5, 28, 27, 7.5, 13, and 22.5 dB at six frequency bands, respectively

Correspondence to:
M. Alibakhshikenari,
alibakhshikenari@ing.uniroma2.it

Citation:
Alibakhshikenari, M., Virdee, B. S., See, C. H., Abd-Alhameed, R. A., Falcone, F., & Limiti, E. (2019). Surface Wave Reduction in Antenna Arrays Using Metasurface Inclusion for MIMO and SAR Systems. *Radio Science*, *54*, 1067–1075. https://doi.org/10.1029/2019RS006871

Received 1 MAY 2019
Accepted 2 OCT 2019
Accepted article online 19 OCT 2019
Published online 21 NOV 2019

Surface Wave Reduction in Antenna Arrays Using Metasurface Inclusion for MIMO and SAR Systems

Mohammad Alibakhshikenari[1], Bal S. Virdee[2], Chan H. See[3,4], Raed A. Abd-Alhameed[5], Francisco Falcone[6], and Ernesto Limiti[1]

[1]Electronic Engineering Department, University of Rome "Tor Vergata", Rome, Italy, [2]Center for Communications Technology and Mathematics, School of Computing and Digital Media, London Metropolitan University, London, UK, [3]School of Engineering and the Built Environment, Edinburgh Napier University, Edinburgh, UK, [4]School of Engineering, University of Bolton, Bolton, UK, [5]Faculty of Engineering and Informatics, University of Bradford, Bradford, UK, [6]Electrical and Electronic Engineering Department, Public University of Navarre, Pamplona, Spain

Abstract An effective method is presented for suppressing mutual coupling between adjacent radiating elements which is based on metasurface isolation for multiple-input multiple-output (MIMO) and synthetic aperture radar (SAR) systems. This is achieved by choking surface current waves induced over the patch antenna by inserting a cross-shaped metasurface structure between the radiating elements. Each arm of the cross-shaped structure constituting the metasurface is etched with meander line slot. Effectiveness of the metasurface is demonstrated for a 2×2 antenna array that operates over six frequency subbands in X, Ku, and K bands. With the proposed technique, the maximum improvement achieved in attenuating mutual coupling between neighboring antennas is 8.5 dB (8–8.4 GHz), 28 dB (9.6–10.8 GHz), 27 dB (11.7–12.6 GHz), 7.5 dB (13.4–14.2 GHz), 13 dB (16.5–16.8 GHz), and 22.5 dB (18.5–20.3 GHz). Furthermore, with the proposed technique (i) minimum center-to-center separation between the radiating elements can be reduced to $0.26\lambda_0$, where λ_0 is 8.0 GHz; (ii) use of ground-plane or defected ground structures are unnecessary; (iii) use of short-circuited via-holes are avoided; (iv) it eliminates the issue with poor front-to-back ratio; and (v) it can be applied to existing arrays retrospectively.

1. Introduction

Minimum spacing between the radiating elements of $0.5\lambda_0$ is normally required for achieving acceptable isolation between elements in microstrip multiple-input multiple-output (MIMO) antenna arrays. Otherwise, the antenna performance is compromised in terms of radiation efficiency, gain, and bandwidth due to the increased electromagnetic (EM) coupling among the closely packed antenna elements resulting from near-field effects.(Ludwig, 1976) Antenna arrays are important in next generation wireless communications systems such as 5G for beam steering andmitigating multipath fading.

Various techniques have been previously explored to reduce mutual coupling between two neighboring patches, for example, by integrating electromagnetic band gap (EBG) structures in patch antenna arrays (Islam & Alam, 2013; Yang et al., 2017; Yang & Rahmat-Samii, 2003) or implementing defected ground structures in the ground-plane.(Chiu et al., 2007; Ghosh & Parui, 2013) Although these techniques are effective in reducing mutual coupling, however, the minimum edge-to-edge spacing between adjacent elements needs to be $0.5\lambda_0$. Waveguided metamaterial is another relatively recent stopband technique(Qamar & Park, 2014) realized by etching metamaterial unit cells in the ground plane under a microstrip line to enhance the current paths in the ground. With this technique edge-to-edge element spacing of $0.125\lambda_0$ can be achieved and the reduction in coupling is confined to only one plane; however, with this approach the impedance bandwidth is limited to 0.02 GHz.

This research work describes a new technique to substantially reduce EM coupling between adjacent radiating elements with reduced center-to-center spacing of $0.26\lambda_0$, where λ_0 is at 8.0 GHz. This is achieved by implementing a metasurface consisting of meander line slot etched inside a microstrip structure, which is inserted between neighboring patches.(Alkurt & Karaaslan, 2019; Bernard et al., 2019; Faenzi et al., 2019; Lin et al., 2019; Ovejero et al., 2018) The proposed metasurface minimizes the effects of EM coupling resulting from space wave and the near field. Compared to other techniques reported in literature, the proposed technique reduces the fabrication process because no ground plane defection or short-circuited via holes

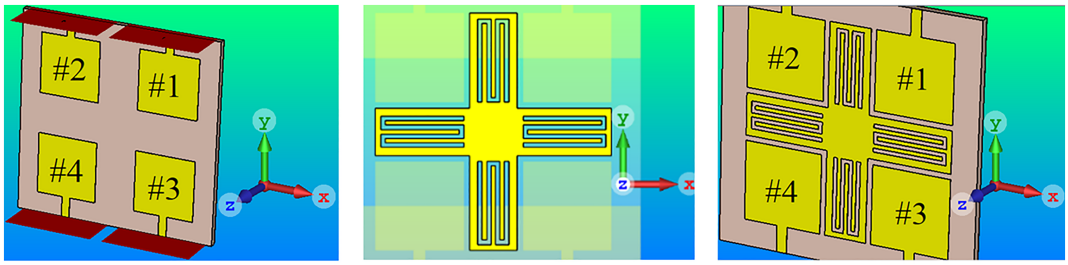

Figure 1. Geometry of the antenna array and proposed metasurface. (a) Reference multiple-input multiple-output 2 × 2 antenna array without metasurface isolator, (b) proposed metasurface isolator implemented using meander line slot, and (c) antenna array with metasurface isolator.

are required, and it eliminates the issue with poor front-to-back ratio. The effectiveness of the proposed technique is validated with measured results. The proposed technique is applied on a wideband antenna operating in X, Ku, and K bands. In X band the application of the antenna is for military communication and wideband global satellite communication systems, in the Ku band it is for terrestrial microwave and radar, specially police traffic speed detector, and in the K band it is for airport surface detection equipment.

2. Metasurface Isolator

The proposed two-dimensional metasurface isolator is constituted by etching a meander line slot (MLS) on a microstrip structure. In Figures 1 and 2, the cross-shaped metasurface is incorporated between adjacent

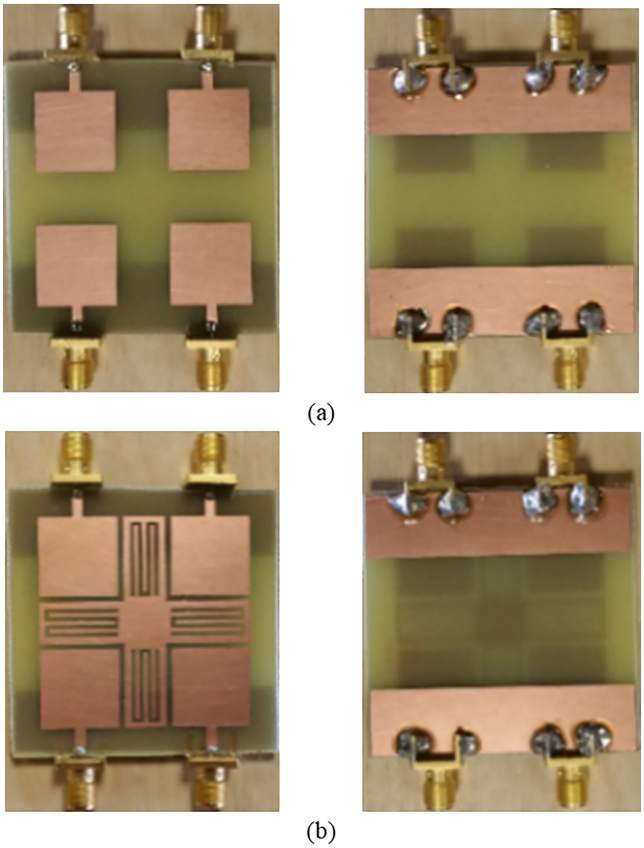

Figure 2. (a) Fabricated prototypes of the antenna array without metasurface isolator (front and back) and (b) fabricated prototypes with metasurface isolator (front and back). Length and width of each patch is 15 mm, and gap between them is 10 mm. Length and width of the meander line metasurface is 61.25 and 0.75 mm, respectively.

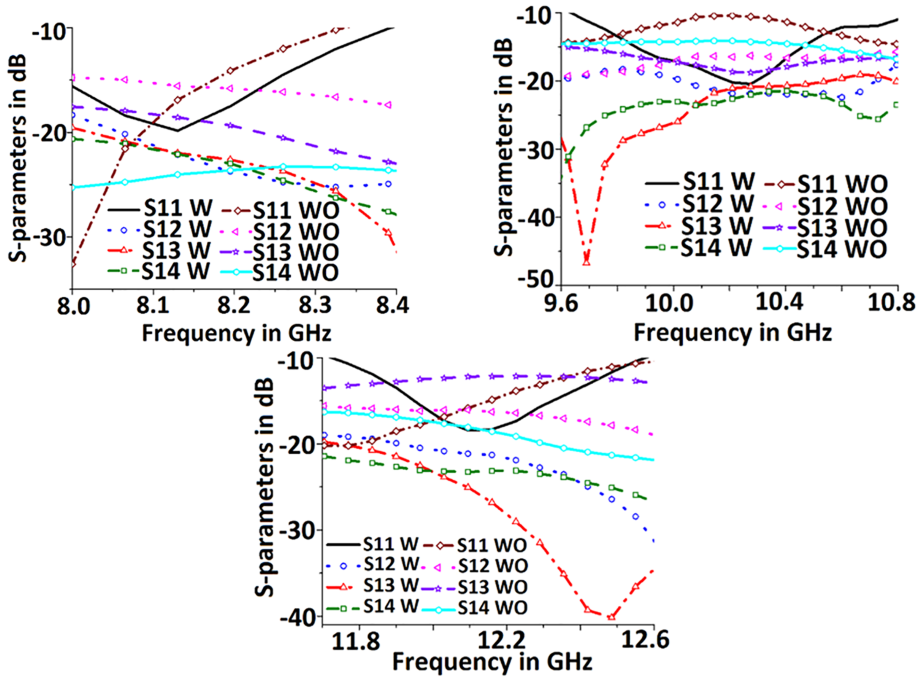

Figure 3. Measured reflection & transmission coefficient responses with (W) and without (WO) metasurface isolator at X and Ku bands.

radiating patches in a 2 × 2 antenna array that has a truncated ground plane. The proposed metasurface essentially chokes surface current waves induced over the antenna by near-field effects thus minimizing EM coupling between the radiating elements. Although not shown the ground planes are common. The antenna array was constructed using a standard Printed Circuit Board (PCB) etching technique on FR-4 dielectric substrate with relative permittivity of 4.3, thickness of 1.6 mm, and loss tangent of 0.025. The square patch has dimensions of 15 × 15 mm^2, and the gap between the patch elements is 10 mm.

The proposed antenna structure in Figure 1 was analyzed using CST-Microwave Studio EM solver, where open (Add Space) boundary condition was applied to create a realistic model. Dimensions of the 2 × 2 antenna array were optimized using CST Microwave Studio to realize maximum bandwidth in the operating frequency bands. Dimensions of the MLS were optimized to realize high isolation between adjacent patches but without significantly affecting the antenna's return loss performance. The length and width of the arms of the cross-shaped isolator are 18.7 and 10.2 mm, respectively. It was observed that the most sensitive part of the proposed MLS to realize high isolation is its length of 62.75 mm and width of 0.75 mm. MLS is not

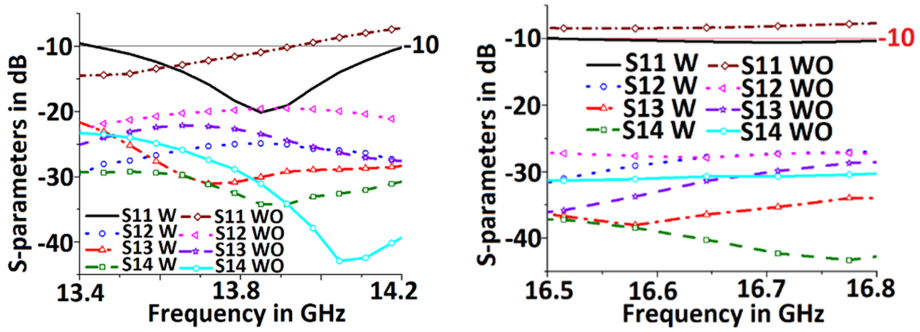

Figure 4. Measured reflection & transmission coefficient responses with (W) and without (WO) metasurface isolator at Ku band.

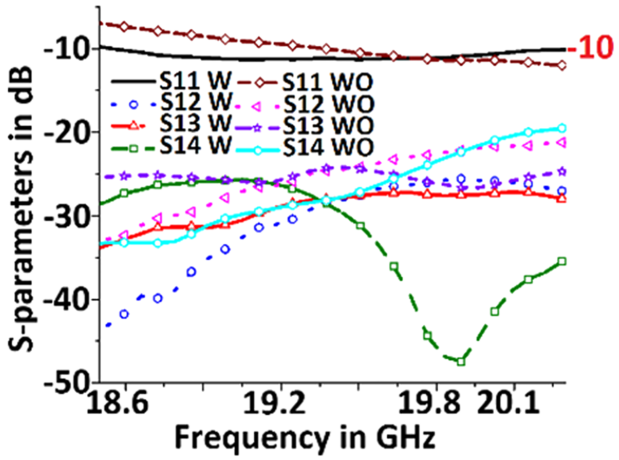

Figure 5. Measured reflection & transmission coefficient responses with (W) and without (WO) metasurface isolator at K band.

implemented in the central section of the cross-shaped isolator because it facilitates electromagnetic interaction with the MLS arms of the cross-shaped structure, thus adversely affecting mutual coupling suppression and therefore the antenna's bandwidth, isolation, and radiation properties. The dimension of this part is 8×8 mm^2. In addition, the length and width of the proposed isolator are 40 and 8 mm, respectively.

Figures 3–5 show the transmission and reflection coefficients of two identical 2×2 antenna arrays, where the reference antenna array has no metasurface. These two parameters were measured using a network analyzer. It is evident that the antenna array with the metasurface exhibits greater isolation than the reference antenna array in the six operating subbands defined for $|S_{11}| \leqq -10$ dB. This is because the metasurface suppresses propagation of surface waves over the antenna and compensates the otherwise out-of-phase radiation from the microstrip patch antennas to improve its reflection coefficient performance. Improvement in the isolation is given in Table 1. It is also evident in Figures 3–5 there is general improvement in the reflection coefficient, too.

The equivalent electrical circuit model of the antenna is shown in Figure 6 where the patch radiator is represented with a resonant circuit comprising inductance L_P, capacitance C_P, and resistance R_P; and where MLS is represented by inductance L_M and capacitance C_M, whose magnitude depends on the gap between the radiators. Coupling between the patch and metasurface isolator is through a combination of L_C and C_C. Inductance L_C is more dominant because the metasurface isolator is coupled via nonradiating edge of the patch antenna. Ohmic and dielectric loss associated with the metasurface isolator is modeled by resistance R_M. Optimized values of the equivalent circuit model given in Table 2 were extracted using Keysight's Advanced Design System (ADS) software tool based on S parameter curves obtained from CST Microwave Studio. The equivalent circuit model was used to determine the effectiveness of the metasurface on the antenna array's return loss and isolation performance. To validate this circuit model, its input impedance was computed using CST Microwave Studio and equivalent circuit model, which are shown in Figure 7.

Table 1
Isolation Improvement With Metasurface

Frequency range (GHz)	$\|S_{12}\|$ (dB)	$\|S_{13}\|$ (dB)	$\|S_{14}\|$ (dB)
	Minimum/maximum/average	Minimum/maximum/average	Minimum/maximum/average
8–8.4	7.5/8.5/8	2/8.5/6	—/3/—
9.6–10.8	2.5/3.5/3	5/28/17	7/18/12.5
11.7–12.6	3.5/13/9.5	8/27/18	5/5/5
13.4–14.2	5.5/7.5/6.5	—/4/2	—/6.5/3.5
16.5–16.8	—/3.5/2	2/5.5/4	7/13/10.5
18.5–20.3	4.5/22.5/13.5	2.5/7.5/5.5	5.5/20/13

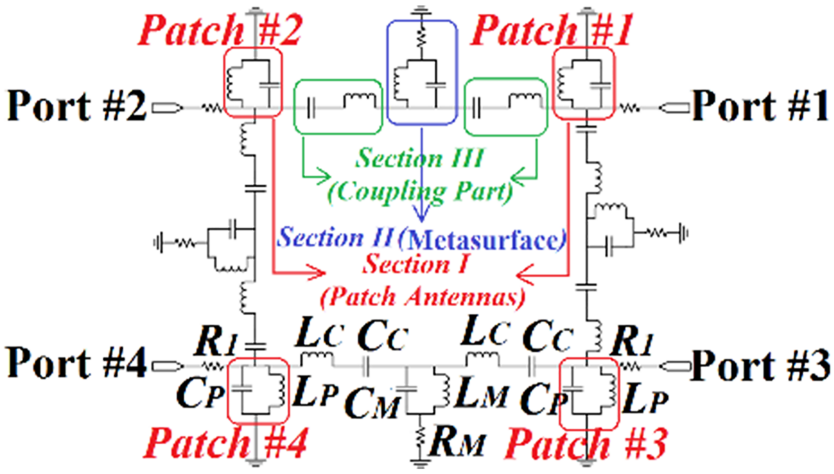

Figure 6. Equivalent circuit diagram of the proposed antenna array.

Radiation patterns of the 2 × 2 antenna array were measured in a standard anechoic chamber by exciting all four elements simultaneously in-phase. Figure 8 shows the simulated and measured radiation characteristics in the vertical plane of the array with and without the metasurface isolator at selected spot frequencies of 8.15, 10.3, 12.15, 13.9, 16.7, and 19.9 GHz across the operating bands. Compared to the reference antenna array, the array with the metasurface structure exhibits reduction in sideband emissions. The discrepancy between simulated and measured results is due manufacturing tolerances and mismatch between the feedline and the antenna.

Decoupling effects can also be observed by visualizing the surface current distribution plots over the 2 × 2 antenna array. With meander line metasurface isolator strong current is induced on the patch antenna and MLS, as shown in Figure 9, which clearly verifies the effectiveness of the meander line metasurface isolator in suppressing surface current wave interaction between the four patches.

The figure of merit for MIMO enabled antenna systems is represented by envelop correlation coefficient (ECC). It can be calculated from measured field patterns by using(Vaughan & Andersen, 1987)

$$\rho_e = \frac{\left|\iint_{4\pi}\vec{E}_1(\theta,\phi)\cdot\vec{E}_2(\theta,\phi)\mathrm{d}\Omega\right|^2}{\iint_{4\pi}\left|\vec{E}_1(\theta,\phi)\right|^2\mathrm{d}\Omega\cdot\iint_{4\pi}\left|\vec{E}_1(\theta,\phi)\right|^2\mathrm{d}\Omega} \tag{1}$$

where

$$\vec{E}_1(\theta,\phi)\cdot\vec{E}_2(\theta,\phi) = \vec{E}^*_{\theta 1}(\theta,\phi)\cdot\vec{E}^*_{\theta 2}(\theta,\phi) + \vec{E}^*_{\phi 1}(\theta,\phi)\cdot\vec{E}^*_{\phi 2}(\theta,\phi) \tag{2}$$

Table 2
Optimized Values of the Equivalent Model Representing the Proposed Structure

Model	Value
C_P	1.0 pF
L_P	7.1nH
R_P	50 Ω
C_M	5.5 pF
L_M	2.8nH
R_M	70 Ω
C_C	8.1 pF
L_C	0.7nH
R_1	75.5 Ω

The term $\vec{E}_1(\theta,\phi)$ is the measured electric field vector radiated by antenna (1), while other antenna ports are terminated with a 50Ω matched load.(Vaughan & Andersen, 1987) The calculated ECCs for the array with and without metasurface are shown in Figure 10. It is evident that by introducing the metasurface, the ECC has improved from 0.35 to less than 0.125. This should result in a higher channel capacity and diversity gain.

3. Comparison With Literature

The proposed antenna array using metasurface is compared in Table 3 with other mutual coupling reduction techniques reported recently. Antenna arrays cited in Table 3 are (i) constructed using two radiation

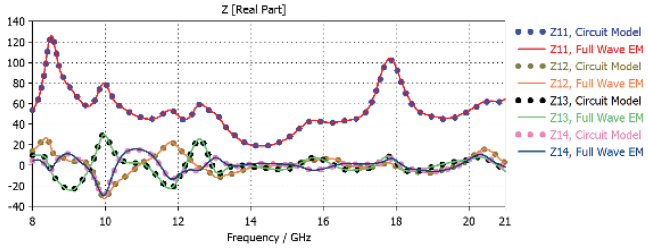

(a) Real part of the input impedance

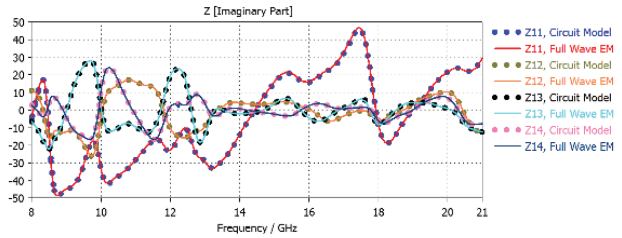

(b) Imaginary Part of the input impedance

Figure 7. Input impedance (Ω) of the proposed antenna array obtained using electromagnetic (EM) simulation and equivalent circuit model.

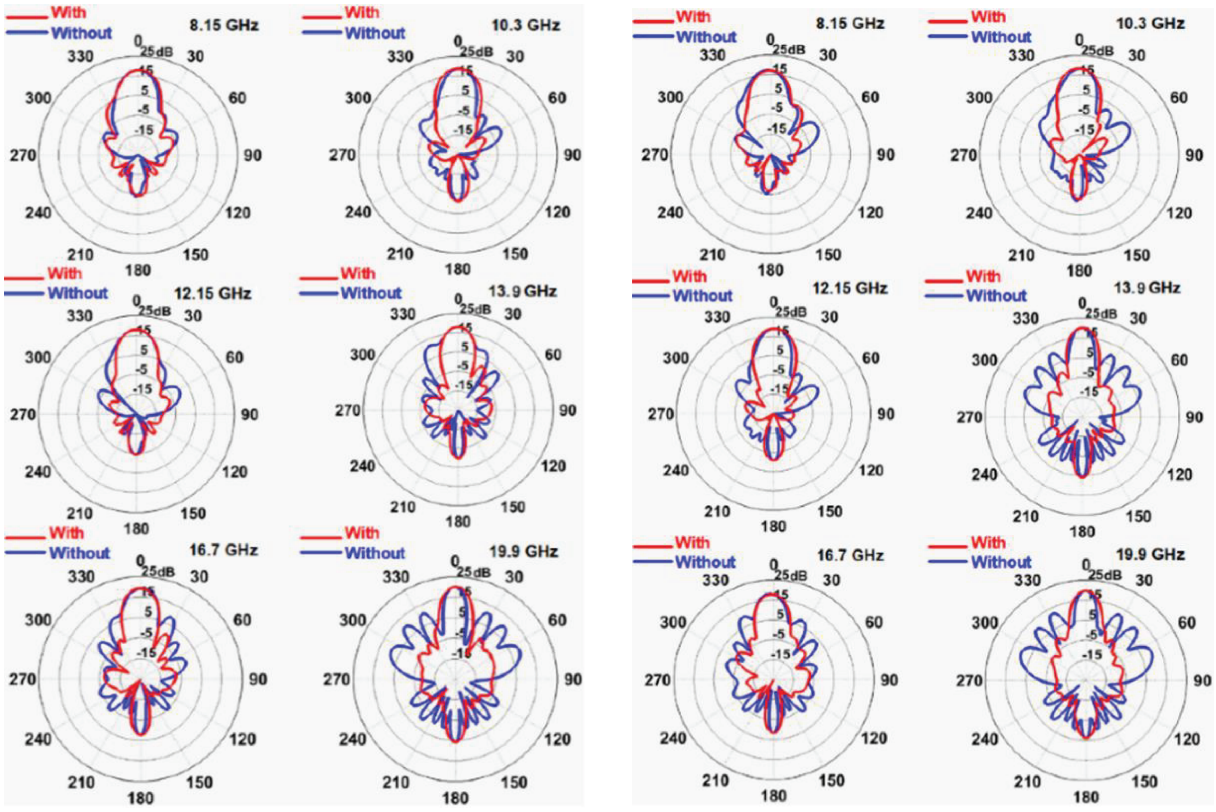

(a) Simulated (b) Measured

Figure 8. Simulated and measured radiation patterns of the reference and proposed antenna arrays at various frequencies of 8.15, 10.3, 12.15, 13.9, 16.7, and 19.9 GHz.

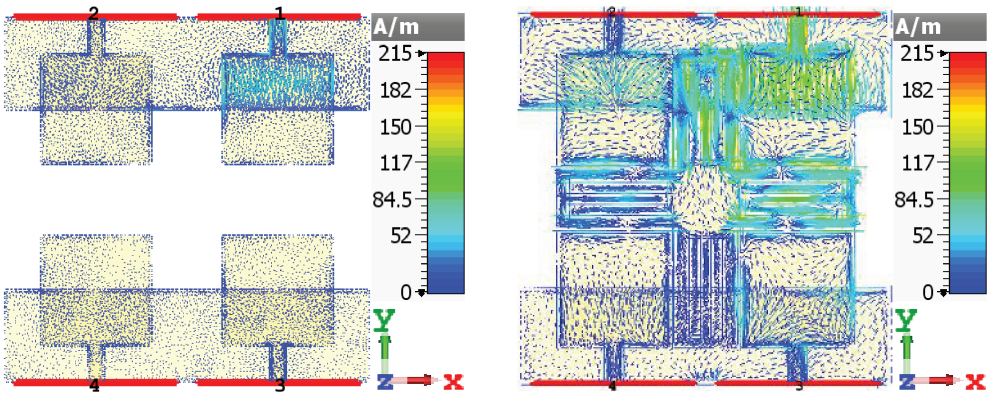

(a) with no metasurface isolator @ 8.15 GHz (b) with meander line metasurface isolator @ 8.15 GHz

Figure 9. Surface current distribution at a spot frequency over the reference antenna array with no metasurface, and over the antenna array with meander line metasurface isolator.

elements, (ii) operated over a narrow and single band, (iii) employed defected ground structure, and (v) exhibit deteriorated radiation patterns. In this paper, we have increased the array elements to four to give a more accurate representation of an array. The proposed method described here offers an optimum isolation between adjacent antennas of 32 dB at X band, 27 dB at Ku band, and 26 dB at K band, which is significantly better than the references cited with exception of.(OuYang et al., 2011) In(OuYang et al., 2011) the authors achieved very good isolation of 40 dB using short-circuited via holes, which is not used in our case, however the antenna operates in a very narrow band. Also, close examination of the decoupling structure in(Alsath et al., 2013) reveals it is based on interdigital capacitance structure not slotted meander line. Compared to the decoupling structure in,(Alsath et al., 2013) the proposed metasurface (i) enables large number of radiation elements to be arranged more compactly in a symmetrical configuration; (ii) exhibits a much wider impedance bandwidth of 5.4 GHz for return loss better than −10 dB, and (iii) isolation improvement on average is 10 dB better over the operating range of the antenna. Furthermore, the proposed technique is simple to implement in practice and can be retrofitted to existing antenna arrays quickly and at low cost. It is important to mention that to achieve high isolation with a simple structure, the proposed array antenna was realized on a truncated ground plane. Unlike other techniques, the proposed technique is relatively easy to design and implement in practice.

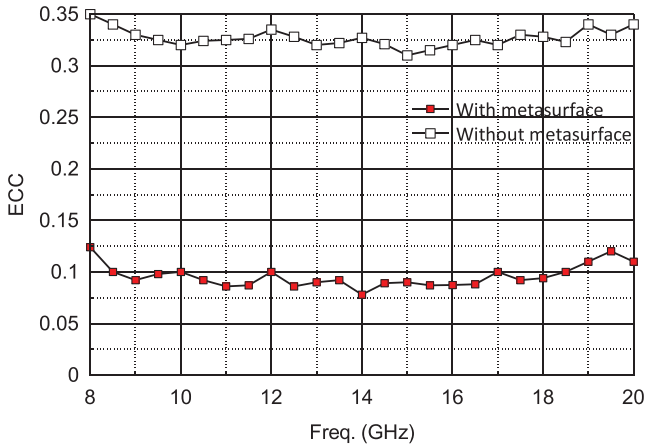

Figure 10. Envelop correlation coefficient (ECC) for the array with and without metasurface.

Table 3
Comparison Between The Proposed Array With The Recent Works

Reference	Method	Maximum isolation	Bandwidth	Bands	Reduction in bandwidth	Radiation pattern deterioration	No. of elements	Use of DGS	Edge-to-edge gap
Yang and Rahmat-Samii (2003)	EBG	8.8 dB	Narrow	Single	Yes	—	2	Yes	$0.75\lambda_0$
Yang et al. (2017)	Fractal load and DGS	16 dB	Narrow	Single	Yes	No	2	Yes	$0.22\lambda_0$
Islam and Alam (2013)	U-shaped resonator	10 dB	Narrow	Single	Yes	Yes	2	Yes	$0.6\lambda_0$
Ghosh and Parui (2013)	I-shaped resonator	30 dB	Narrow	Single	Yes	Yes	2	Yes	$0.45\lambda_0$
Qamar and Park (2014)	W/g Metamaterial (MTM)	18 dB	Narrow	Single	Yes	No	2	Yes	$0.093\lambda_0$
OuYang et al. (2011)	Ground slot	40 dB	Narrow	Single	Yes	Yes	2	Yes	$0.23\lambda_0$
Zhu et al. (2012)	slotted-complementary split-ring resonators (SCSRR)	10 dB	Narrow	Single	Yes	Yes	2	Yes	$0.25\lambda_0$
Suwailam et al. (2010)	SCSSRR	14.6 dB	Narrow	Single	Yes	Yes	2	Yes	$0.125\lambda_0$
Shafique et al. (2015)	Compact EBG	17 dB	Narrow	Single	Yes	Yes	2	Yes	$0.8\lambda_0$
Farsi et al. (2012)	Meander line	10 dB	Narrow	Single	Yes	No	2	Yes	$0.055\lambda_0$
Ghosh et al. (2016)	UC-EBG	14 dB	Narrow	Single	Yes	Yes	2	Yes	$0.5\lambda_0$
Farahani et al. (2010)	EBG	10 dB	Narrow	Single	Yes	Yes	2	Yes	$0.5\lambda_0$
Rajo-Iglesias et al. (2008)	EBG	5 dB	Medium	Single	Yes	—	2	Yes	$0.6\lambda_0$
Al-Hasan et al. (Feb. 2015)	EBG	13 dB	Medium	Single	Yes	Yes	2	Yes	$0.5\lambda_0$
Exposito-Dominguez et al. (2012)	EBG and DGS	16 dB	Narrow	Single	Yes	No	2	Yes	$0.6\lambda_0$
Yu and Zhang (2003)	EBG	4 dB	Narrow	Single	Yes	Yes	2	Yes	$0.84\lambda_0$
Alsath et al. (2013)	Slotted meander line	16 dB	Narrow	Single	Yes	Yes	2	No	$0.11\lambda_0$
Yang et al. (2012)	W/g MTM	20 dB	Narrow	Single	Yes	No	2	Yes	$0.125\lambda_0$
This work	Metasurface	32 dB (X band) 27 dB (Ku band) 26 dB (K band)	Cumulative Bandwidth (BW) is 5.4 GHz	Six	No	No	4	No	$0.26\lambda_0$

Note. EBG = electromagnetic band gap; DGS = defected ground structures.

4. Conclusion

A novel metasurface is shown to effectively isolate electromagnetic coupling between neighboring antenna elements. Surface current waves over the patch antenna are suppressed by locating the cross-shaped metasurface between the radiating elements in the 2×2 antenna array. The proposed technique permits reduction in centre-to-centre separation between antenna radiating elements to $0.26\lambda_0$, where $\lambda_0$is 8.0 GHz, does not require short-circuited via holes or defected ground structures and can be retrofitted. Over its operating range the proposed technique offers an optimum isolation between adjacent antennas of 32 dB at X band, 27 dB at Ku band, and 26 dB at K band. The technique presented enables implementation of densely packed antenna arrays in MIMO and synthetic aperture radar systems.

Acknowledgments
This work is partially supported by innovation programme under grant agreement H2020-MSCA-ITN-2016 SECRET-722424 and the financial support from the UK Engineering and Physical Sciences Research Council (EPSRC) under grant EP/E022936/1. The authors confirm that there is no relevant domain or general repository for the data. The authors have arranged for all data to be contained in the manuscript (not a repository) for reviewers and readers to access them, and the section affirms this.

References

Al-Hasan, M. J., Denidni, T. A., & Sebak, A. R. (Feb. 2015). Millimeter wave compact EBG structure for mutual coupling reduction applications. *IEEE Transactions on Antennas and Propagation*, *63*(2), 823–828.

Alkurt, F. O., & Karaaslan, M. (2019). Pattern reconfigurable metasurface to improve characteristics of low profile antenna parameters. *International Journal of RF and Microwave Computer-Aided Engineering*, e21790. https://doi.org/10.1002/mmce.21790

Alsath, M. G., Kanagasabai, M., & Balasubramanian, B. (2013). Implementation of slotted meander line resonators for isolation enhancement in microstrip patch antenna arrays. *IEEE Antennas and Wireless Propagation Letters*, *12*, 15–18.

Bernard, L., Martinis, M., Collardey, S., Mahdjoubi, K., & Sauleau, R. (2019). Metasurface antennas embedded in small circular cavities for telemetry applications. *Applied Sciences*, *9*(12).
Chiu, C. Y., Cheng, C. H., Murch, R. D., & Rowell, C. R. (2007). Reduction of mutual coupling between closely-packed antenna elements. *IEEE Transactions on Antennas and Propagation*, *55*(6), 1732–1738.
Exposito-Dominguez, G., Fernandez-Gonzalez, J. M., Padilla, P., & Sierra-Castaner, M. (2012). Mutual coupling reduction using EBG in steering antennas. *IEEE Antennas and Wireless Propagation Letters*, *11*, 1265–1268.
Faenzi, M., Minatti, G., Gonzalez-Ovejero, D., Caminita, F., Martini, E., Della Giovampaola, C., & Maci, S. (2019). Metasurface antennas: New models, applications and realizations. *Scientific Reports*, *9*(1), 1–14.
Farahani, H. S., Veysi, M., Kamyab, M., & Tadjalli, A. (2010). Mutual coupling reduction in patch antenna arrays using a UC-EBG superstrate. *IEEE Antennas and Wireless Propagation Letters*, *9*, 57–59.
Farsi, S., Schreurs, D., & Nauwelaers, B. (2012). Mutual coupling reduction of planar antenna by using a simple microstrip U-section. *IEEE Antennas and Wireless Propagation Letters*, *11*, 1501–1503.
Ghosh, C. K., & Parui, S. K. (2013). Reduction of mutual coupling between E-shaped microstrip antennas by using a simple microstrip I-section. *Microwave and Optical Technology Letters*, *55*(11), 2544–2549.
Ghosh, J., Ghosal, S., Mitra, D., Ranjan, S., & Chaudhuri, B. (2016). Mutual coupling reduction between closely placed microstrip patch antenna using meander line resonator. *Progress in Electromagnetic Research Letters*, *59*, 115–122.
Islam, M. T., & Alam, M. S. (2013). Compact EBG structure for alleviating mutual coupling between patch antenna array elements. *Progress in Electromagnetics Research*, *137*, 425–438.
Lin, F.H., Li, T. and Chen, Z.N., "Recent progress in metasurface antennas using characteristic mode analysis,"13th European Conference on Antennas and Propagation (EuCAP), 31 March-5 April 2019, Krakow, Poland. (2019)
Ludwig, A. (1976). Mutual coupling, gain and directivity of an array of two identical antennas. *IEEE Transactions on Antennas and Propagation*, *42*(6), 837–841.
OuYang, J., Yang, F., & Wang, Z. M. (2011). Reduction of mutual coupling of closely spaced microstrip MIMO antennas for WLAN application. *IEEE Antennas and Wireless Propagation Letters*, *10*, 310–312.
Ovejero, D.G., Morvan, X., Chahat, N., Chattopadhyay, G., Sauleau, R. and Ettorre, M., "Metallic metasurface antennas for space," 12th European Conference on Antennas and Propagation (EuCAP 2018), 2018.
Qamar, Z., & Park, H.-C. (2014). Compact waveguided metamaterials for suppression of mutual coupling in microstrip array. *Progress in Electromagnetics Research*, *149*, 183–192.
Rajo-Iglesias, E., Quevedo-Teruel, O., & Inclan-Sanchez, L. (2008). Mutual coupling reduction in patch antenna arrays by using a planar EBG structure and a multilayer dielectric substrate. *IEEE Transactions on Antennas and Propagation*, *56*(6), 1648–1655.
Shafique, M. F., Qamar, Z., Riaz, L., Saleem, R., & Khan, S. A. (2015). Coupling suppression in densely packed microstrip arrays using metamaterial structure. *Microwave and Optical Technology Letters*, *57*(3), 759–763.
Suwailam, M. M. B., Siddiqui, O. F., & Ramahi, O. M. (2010). Mutual coupling reduction between microstrip patch antennas using slotted-complementary split-ring resonators. *IEEE Antennas and Wireless Propagation Letters*, *9*, 876–878.
Vaughan, R. G., & Andersen, J. B. (1987). Antenna diversity in mobile communications. *IEEE Transactions on Vehicular Technology*, *36*(4), 147–172.
Yang, F., & Rahmat-Samii, Y. (2003). Microstrip antennas integrated with electromagnetic band-gap (EBG) structures: A low mutual coupling design for array applications. *IEEE Transactions on Antennas and Propagation*, *51*(10), 2936–2946.
Yang, X., Liu, Y., Xu, Y.-X., & Gong, S.-X. (2017). Isolation enhancement in patch antenna array with fractal UC-EBG structure and cross slot. *IEEE Antennas and Wireless Propagation Letters*, *16*, 2175–2178.
Yang, X. M., Liu, X. G., Zhu, X. Y., & Cui, T. J. (2012). Reduction of mutual coupling between closely packed patch antenna using waveguide metamaterials. *IEEE Antennas and Wireless Propagation Letters*, *11*, 389–391.
Yu, A., & Zhang, X. (2003). A novel method to improve the performance of microstrip antenna arrays using a dumbbell EBG structure. *IEEE Antennas and Wireless Propagation Letters*, *2*(1), 170–172.
Zhu, F. G., Xu, J. D., & Xu, Q. (2012). Reduction of mutual coupling between closely packed antenna elements using defected ground structure. *Electronics Letters*, *45*(12), 601–602.